THE DECAY SCHEME OF SE^{75}

by

HARVEY ROY SCHNEIDER

A THESIS SUBMITTED IN PARTIAL FULFILMENT OF THE
REQUIREMENTS FOR THE DEGREE OF

MASTER OF ARTS

in the Department

of

Physics

We accept this thesis as conforming
to the standard required from candidates for the degree of MASTER OF ARTS

THE UNIVERSITY OF BRITISH COLUMBIA

1957

A B S T R A C T

Excited levels of As^{75} were investigated by studying the decay of Se^{75}. Scintillation detection techniques were employed to measure, the relative gamma ray intensities, gamma-gamma coincidences, and conversion electron-gamma coincidences. A decay scheme with five excited As^{75} levels at 200, 265, 280, 305 and 402 kev. is proposed. Multipolarities are assigned to the transitions between these levels on the basis of conversion coefficients, determined from previously measured conversion intensities.

In presenting this thesis in partial fulfilment of the requirements for an advanced degree at the University of British Columbia, I agree that the Library shall make it freely available for reference and study. I further agree that permission for extensive copying of this thesis for scholarly purposes may be granted by the Head of my Department or by his representative. It is understood that copying or publication of this thesis for financial gain shall not be allowed without my written permission.

Department of Physics

The University of British Columbia,
Vancouver 8, Canada.

Date 18 April 1957

ACKNOWLEDGMENT

The research described in this thesis has been made possible through a Grant-in-Aid-of-Research to Dr. K.C. Mann, by the National Research Council.

The author wishes to express his sincere thanks to Dr. K.C. Mann for his guidance and assistance throughout this work.

TABLE OF CONTENTS

TABLE OF ILLUSTRATIONS

1. INTRODUCTION.

It has been well established that the constituents of the atomic nucleus, called nucleons, are of two types, protons and neutrons. These particles have very nearly the same mass, one atomic mass unit, but differ in regard to electro static charge and magnetic moment; the proton being positively charged and having a magnetic moment of 2.79 nuclear magnetons, while the neutron is uncharged and has a magnetic moment of -1.91 nuclear magnetons. The number of protons in a nucleus (the atomic number) is denoted by Z and the number of neutrons by N. A shorthand method for indicating the composition of a nucleus is as follows:

$$ {}_{Z}X_{N}^{A} $$

Where X is the chemical symbol corresponding to Z and A is the atomic mass number, which is equal to N + Z.

Quantum mechanical arguments applied to the neutron-proton system comprising the nucleus, show that such a system can exist only in discrete energy states. When the nucleus possesses minimum energy it is said to be in its ground state; all other possible energy states are called excited states. In addition to energy, each state is characterized by an angular momentum quantum number (spin) and a parity. The spin gives the total angular momentum of the nucleus in units of $\hbar$, while the parity defines the symmetry properties of the wave function which describes the state.

The parity may be either even (+) or odd (-) depending upon whether the wave function is symmetric or anti-symmetric with respect to a reflection of the coordinate system.

Certain nuclei are energetically unstable against decay to other nuclei. The condition for instability depends upon the masses involved and may be expressed as follows: Suppose that "a" represents a nucleus of Z protons and N neutrons, let M(a) represent the mass of this nucleus "a". Now consider the N + Z particles being redistributed among particles "b" and "c", where M(b) and M(c) represent the masses of these particles measured separately. Then if, $M(a) > M(b) + M(c)$, particle "a" is energetically unstable against spontaneous decay to "b" and "c". The difference in the masses of the two nucleon arrangement usually appears as kinetic energy of the particles "b" and "c". If one plots the atomic mass versus Z for a typical group of isobaric nuclei (i.e. nuclei with same A but different Z) with odd A say, a curve such as that in figure 1 is obtained. In this case nucleus 3 is stable while nuclei 1, 2, 4 and 5 are energetically unstable against decay to the lower masses. This instability usually results in the spontaneous change of charge of the nucleus through beta decay. That is, nucleus 1 decays to nucleus 2 by emitting a negative electron (negatron) and 2 decays 3 by a similar process.

We describe this process as being caused by the spontaneous decay of one of the nuclear neutrons into a proton and a negatron. This event

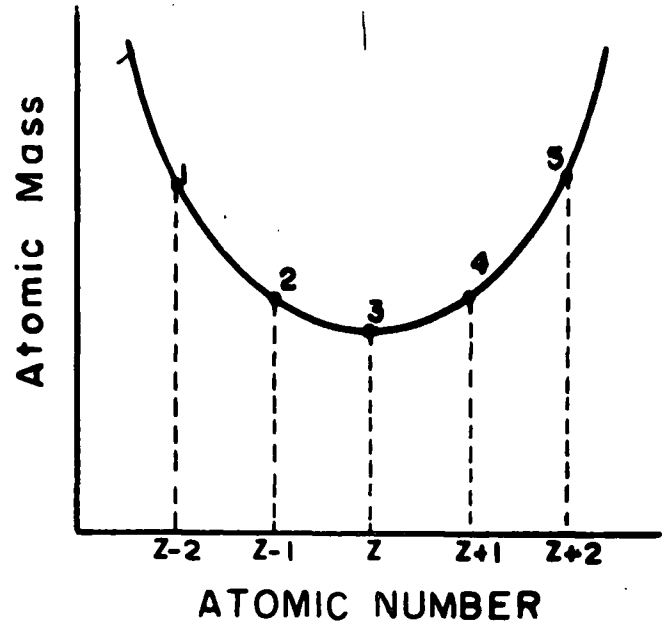

Relationship between A and Z for odd A isobars

Figure 1

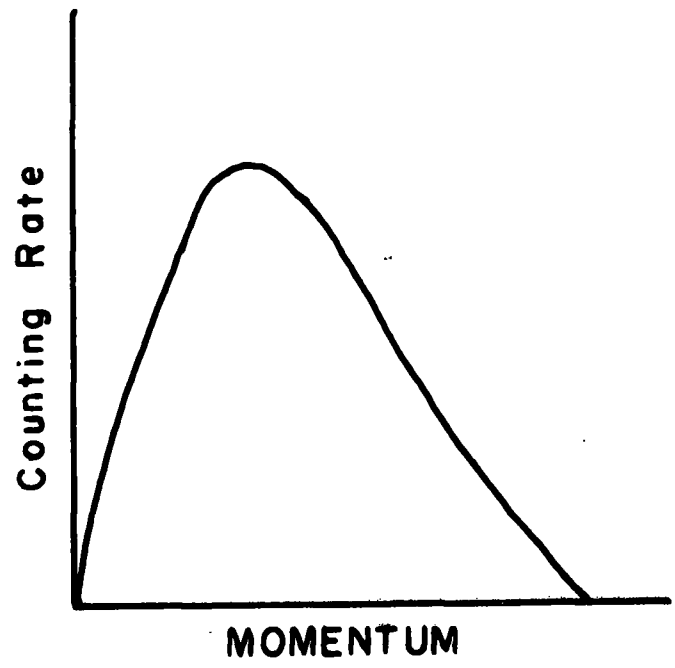

A typical primary beta spectrum

Figure 2

then changes the atomic number of the nucleus from Z to Z + 1, but of course the mass A remains unchanged. Thus all beta decay process take place between isobars.

For the decay of nuclei 5 to 4 to 3, two processes are possible; either the nucleus decays by emitting a positive electron (positron) or it decays by capturing an orbital electron. This process is defined as the reverse of negatron emission; a nuclear proton converts to a neutron by emitting a positron or absorbing a negative orbital electron. Thus there results a change of atomic number from Z to Z-1 in either case, and as before A remains unchanged.

Each of these beta decay processes require a certain amount of energy before they can occur. This minimum energy requirement, expressed in terms of <u>atomic</u> masses of the parent and daughter atoms is given in Table 1.

Table 1

Parent		Daughter
M_{at} (Z-1, N+1)	>	M_{at} (Z,N) for β^- decay.
M_{at} (Z+1,N-1)	>	M_{at} (Z,N) + 2 m_e for β^+ decay.
M_{at} (Z+1, N-1)	>	M_{at} (Z,N) for orbital electron capture.

Where m_e is the mass of the electron.

The momentum distribution of particle radiations occuring in beta decay have been analyzed for a large number of radioactive nuclides using

a variety of spectrometers and nuclear spectro scopic techniques. In every case it is found that the beta particles are emitted with a continuous momentum (and hence also energy) distribution from zero up to some maximum. An example of the type of beta spectrum one obtains is shown in figure 2.

The maximum energy with which a beta particle is emitted is equal to the energy difference between the parent and daughter nuclei as given in Table 1. When the beta particle is emitted with an energy less than the maximum however, there appears to be a violation of the law of conservation of energy, since no other particle is observed which, together with the beta emission, would account for the total disintegration energy. Another difficulty arises from angular momentum considerations. Protons, neutrons and electrons have intrinsic spins of $\frac{1}{2}\hbar$ and obey Fermi statistics. Thus even A nuclei must have integral values of total spin while odd A nuclei must have odd half-integral total spins. Since beta decay takes place between isobars, any spin change between parent and daughter nucleus must be integral or zero. Now if the decay radiation consists of only one electron, then the total spin change must always be odd half-integral. Thus the law of conservation of angular momentum appears not to hold.

In order to reestablish the validity of the conservation laws, Pauli in 1927 postulated the simultaneous emission of a second particle, the neutrino, in beta decay processes. To agree with observation this

particle must have zero charge and a very small (probably zero) mass. Then the conservation laws are satisfied if the neutrino has a spin of $\frac{1}{2}\hbar$ and shares the disintegration energy with the electron in beta decay. In the case of decay by orbital electron capture, the neutrino carries away the entire disintegration energy, since there are no primary charged particles emitted. The properties of the neutrino admit very little interaction with matter. For this reason, attempts at direct detection of the particle have not been successful, although certain measurements on the recoil momentum of the daughter nucleus and the emitted electron are consistent with the postulate of the neutrino.

Fermi Theory of Beta Decay

(1) Momentum Distribution.

Among the early evidence supporting the neutrino hypothesis was the success of Fermi's theory of beta decay.[1] According to this theory the continuous beta spectrum results from a statistical sharing of the disintegration energy by the electron and neutrino. This means that both the electron and neutrino energies (and hence also momenta) are statistically distributed, subject however to the condition:

$$E_{max} = E_\beta + E_\nu \qquad (1)$$

Where, Emax is the disintegration energy, E_β and E_ν are the neutrino and beta particle energies respectively. The distribution of the momenta of

the emitted beta particles is predicted by this theory, to be:

$$P(p)\,dp = k\,|H_{fi}|^2\,p^2\,(E_{max} - E)\,F(z,p)\,dp \qquad (2)$$

Where, $P(p)dp$ is the probability that a beta particle will be emitted with momentum between p and $p + dp$; k is a constant; $|H_{fi}|^2$ is a transition matrix describing the probability that a nucleus will undergo beta decay; and $F(z,p)$ is the Fermi function, a complex function that corrects the momentum distribution for the effect of the nuclear coulomb field on the beta particle. The Fermi function has been evaluated and tabulated [2] for Z = 1 to 100 and a wide range of p.

Decays involving no change in orbital angular momentum ($\Delta l = 0$) of the nucleus are called allowed, while decays for which $\Delta l \neq 0$ are called forbidden transitions. The matrix element $|H_{fi}|^2$ is independent of the beta ray energy for allowed decays, but this is not, in general, true for forbidden decays. Consequently the shape of beta spectra for forbidden transitions are usually different from those for allowed transitions.

(2) Selection Rules.

The selection rules to be used to determine nuclear spin and parity changes resulting from beta decay depend upon whether the neutrino and electron are emitted with parallel or anti parallel spins.

The assumption of parallel spins results in Gamow-Teller selection rules, whereas anti parallel spins result in Fermi selection rules: see

Table 2:

Table 2

Transition Classification	Fermi ΔI	Fermi $\Delta \pi$	Gamow-Teller ΔI	Gamow-Teller $\Delta \pi$
Allowed	0	No	$0, \pm 1$ (not $0 \to 0$)	No
1st Forbidden	$0, \pm 1$ (not $0 \to 0$)	Yes	$0, \pm 1, \pm 2$ (not $0 \to 0$) ($\frac{1}{2} \to \frac{1}{2}$)	Yes
2nd Forbidden	$\pm 1, \pm 2$ (not $0 \leftrightarrow 1$)	No	$\pm 2 \pm 3$ (not $0 \leftrightarrow 2$)	No

(3) Comparative Half Life.

By integrating equation (2) we get the total probability of decay per unit time,

$$\lambda = k |H_{fi}|^2 \int_0^{p_{max}} F(z,p)\, p^2\, (E_{max} - E)\, dp \qquad (3)$$

λ is related to the half life of the decay by,

$$\lambda = \frac{\log 2}{T_{\frac{1}{2}}} \qquad (4)$$

Therefore from equations (3) and (4) we get,

$$\frac{\log 2}{T_{\frac{1}{2}}} = k |H_{fi}|^2 f(z, E_{max}) \qquad (5)$$

Where $f(z, E_{max})$ is the value of the integral in equation (3). Finally rewriting equation (5) gives

$$f\, T_{\frac{1}{2}} \propto \frac{1}{|H_{fi}|^2} \qquad (6)$$

f $T_{\frac{1}{2}}$ is known as the comparative half life of the transition. Its value is of assistance in determining whether a transition is allowed or to what degree it is forbidden.

Since $|H_{fi}|^2$ decreases very rapidly with increasing forbiddeness, it is necessary to consider only the order of $fT_{\frac{1}{2}}$ to indicate the class of the transition. Hence it is customary to use $\log_{10}fT_{\frac{1}{2}}$ values. If both the energy and the half life of the decay are known, the $\log_{10}fT_{\frac{1}{2}}$ value may in principle be calculated. The computations are difficult and fortunately nomographs based on such calculations are available[3]. Approximate ranges of $\log_{10}fT_{\frac{1}{2}}$ values for the first three classes of beta transitions are given in Table 3:

Table 3

Classification	Approximate $\log_{10}fT_{\frac{1}{2}}$ value.
Allowed	3 - 6
1st Forbidden	6 - 10
2nd Forbidden	10

On the basis of $\log_{10}fT_{\frac{1}{2}}$ values alone one cannot unambiguously determine the classification of a beta transition, since there is some overlap of the values from one class to another.

(4) K - Capture.

The decay probability given in equation (3) applies only to decays involving the simultaneous emission of a beta particle and a neutrino. When the nucleus decays by orbital electron capture, however, certain modi-

fications are necessary; for example, since the neutrino is the only particle emitted the factors expressing the statistical sharing of energy between the beta particle and neutrino do not appear.

Also, to obtain equation (2) plane wave approximations for the electron and neutrino were used. For orbital electron capture processes the wave function of the capture electron - usually one of the k shell electrons - is used. With these modifications the total decay probability for k-capture may be written as:

$$\lambda_k = |H_{fi}|^2 f_k (z, E_{max}) \qquad (7)$$

In this case E_{max} is the maximum energy of the emitted neutrino, and consequently if is not as easily determined as in the case of beta particle emission. As before, we can write equation 7 as follows:

$$f_k T_{\frac{1}{2}} \propto \frac{1}{|H_{fi}|^2} \qquad (8)$$

Nomographs for $\log_{10} f_k (z, E_{max})$ have also been prepared by Moszkowski.[3]

Nuclear Decay Schemes.

A nucleus resulting from a decay process is frequently left in an excited state. Such a nucleus will tend to drop to lower levels of excitation and ultimately to the ground state, usually through one of two competing processes. These two deexcitation processes are, emission of a photon (gamma ray), and direct transfer of the excitation energy to an orbital electron which is then emitted with an energy equal to the trans-

ition energy minus the binding energy of the electron. The latter process is called internal conversion.

The decay and subsequent deexcitation of a nucleus is conveniently represented by a diagram called a decay scheme, see for example figure 3. I_a, I_b, I_c in figure 3 refer to the spins of the corresponding states and E_1, E_2 are the excitation energies.

Multipole Radiation.

Gamma radiation is classified by multipole orders L, according to the angular momentum (in units of $\hbar$) carried off by the photon. For each multipole order there are two classes of radiation; electric multipole and magnetic multipole, which differ with respect to parity changes. Electric dipole, quadrapole, octupole, etc. radiations are usually denoted by the symbols, E1, E2, E3, E4, etc. Where the multipolarity is determined from 2^L . Similarly M1, M2, etc. denote magnetic multipole radiations. Selection rules governing the possible multipolarities for a specific transition between two states with spins J_i and J_f are:

$$|J_i - J_f| \leq L \leq J_i + J_f$$

$\Delta\pi = (-1)^L$ for electric multipole radiation

$\Delta\pi = (-1)^{L-1}$ for magnetic multipole radiation

If $J_i = J_f = 0$ then a gamma transition is strictly forbidden. Since the transition probability decreases with increasing multipolarity, one expects only the lowest multipole order permitted by the selection rules ($L=|J_i - J_f|$),

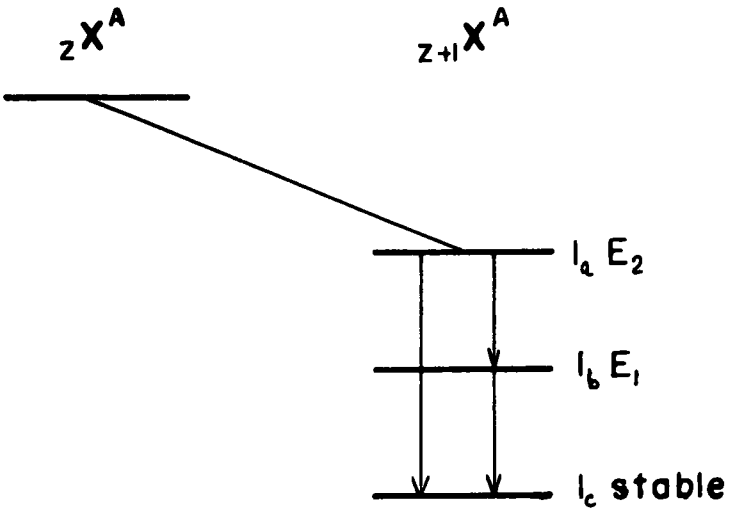

A Typical Decay Scheme

Figure 3

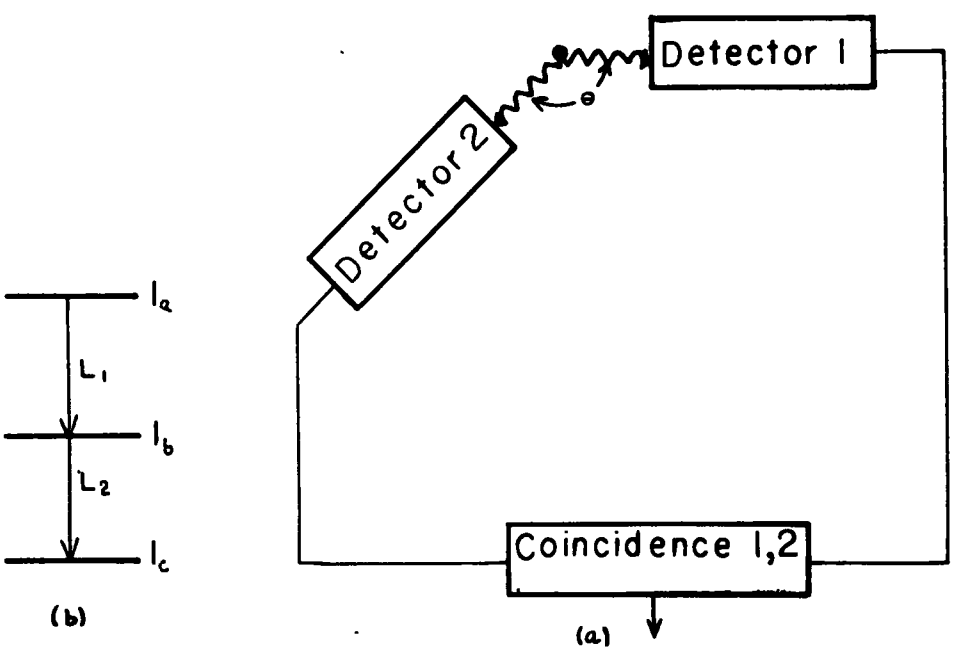

Basic Angular Correlation System

Figure 4

or perhaps in some cases a mixing of the two lowest multipolarities (but of opposite class because of parity considerations).

There are several different measurements from which the multipole orders of gamma transitions can be deduced. Some of these are described below.

(1) Conversion Coefficient:

If λ_γ and λ_e are the probabilities of gamma and conversion electron emission respectively, for a particular nuclear transition, then we define the total conversion coefficient for this transition as:

$$\alpha = \frac{\lambda_e}{\lambda_\gamma} \qquad (9)$$

In the majority of cases conversion electrons from innermost (k) shell are the most intense, hence often it is more useful to consider the k - conversion coefficient.

$$\alpha_k = \frac{\lambda_k}{\lambda_\gamma} \qquad (10)$$

Where λ_k is the relative probability of emission of a k conversion electron. Values of conversion coefficients depend upon (1) the energy of the transition, (2) the atomic number of the nucleus, (3) the shell from which the electron is ejected, (4) the multipolarity of the competing gamma transition and (5) the character of the nuclear transition i.e. either electric or magnetic. Theoretical K and L shell conversion coefficients have been calculated and tabulated by Rose[4] et al for both electric and magnetic transitions with multipolarities up to 2^5. By comparing the experimental conversion co-

efficient with these calculations it is usually possible to establish the multipolarity and the character of the transition.

(2) K/L Ratio.

When the intensities of both the K and L conversion transitions can be measured the corresponding multipolarities may be determined from the ratio of these intensities since

$$K/L = \frac{\alpha_K}{\alpha_L} = \frac{\lambda_K}{\lambda_L} \qquad (11)$$

Where K/L is the intensity ratio of the K and L conversion lines. This method is sometimes preferred over method(1) since it does not involve direct measurement of gamma-ray intensities. Empirical curves of K/L ratios to determine multipolarities are given by Goldhaber and Sunyar.[10]

(3) Angular Correlation:

The probability of emission of a photon from a nucleus depends in general upon the angle between the direction of emission and the nuclear spin axis. The actual form of the probability function being determined by the nuclear spin change and the multipolarity of the gamma transition. Despite this angular dependence of the emission probability, gamma radiation from ordinary radio active sources is observed to be isotropic, because nuclei making up the source are randomly oriented. If, however, it is possible to detect only the radiation from those nuclei oriented in a particular fashion while excluding the radiations from all other nuclei, then we would

again have an anisotropic distribution. Using coincidence counting techniques such a selection is possible for cases where there are two gamma rays in cascade. Consider for example, a detection system as shown in figure 4a which is used to study the cascade shown in figure 4b.

Detection of L_1 establishes a reference direction, i.e. only coincident radiation from nuclei oriented in a particular fashion is detected, and therefore the second gamma ray L_2 will have an angular correlation with respect to the first. The assumption here is, of course, that the lifetime of the intermediate state is short enough to allow no reorientation of the nucleus between emission of L_1 and L_2.

The theoretical correlation function is of the form[5],

$$W(\theta) = \sum_{\nu=0}^{\nu_{max}} A_\nu P_\nu (\cos\theta) \qquad (12)$$

$$0 \leq \nu_{max} \leq \text{Min } (2I_4, 2L_1, 2L_2)$$

Where, $W(\theta)d\Omega$ is the relative probability that L_2 will be emitted into a solid angle $d\Omega$ at an angle θ with respect to L_1. The values of the coefficients A_ν depend upon the spins of the three states involved as well as the multipolarities of the gamma transitions. Theoretical values for A_ν have been calculated and tabulated by Rose et al[6] for various combinations of spins and multipolarities.

Nuclear Models.

The lack of a complete nuclear theory has resulted in the development of various nuclear models, which are used as an aid in interpreting the

data obtained from nuclear experiments.

(1) Shell Model.

A surprisingly successful account of a great variety of nuclear phenomena is obtained through the use of the nuclear shell model ; developed by Mayer et al[7]. For this model it is assumed that nucleons move in orbits within the nucleus, analagous to electronic motion in orbits in the atom. It is further assumed that the motion of any particular nucleon can be determined by considering it to be moving in an average static nuclear potential, due to all the other nucleons in the nucleus. Then the internal motion of the nucleus is obtained by a super position of all the quasi independent motions of the individual nucleons.

Each nucleon orbit is characterized by quantum numbers which determine a nuclear energy level. According to the Pauli principle these levels may be filled with neutrons and protons independently. Whenever two successive groups of levels are widely separated and the lower group is completely populated, there is said to be a shell closure at the separation. Nuclei with all nucleons in closed shells are exceptionally stable. Such exceptional stability has been observed for nuclei with 2, 8, 20, 50, 82 and 126 identical nucleons. In order to predict shell closures at these nucleon numbers, Mayer et al assumed strongspin orbit coupling. Thus a level with angular momentum l splits into two levels, one with total angular momentum $j = l + \frac{1}{2}$ and the other with $j = l - \frac{1}{2}$.

The level with $j = \ell + \frac{1}{2}$ is the lower one, and the separation from the other is proportional to $2\ell + 1$ (i.e. the splitting increases with ℓ).

Nuclear spins and magnetic moments are predicted by the shell model, if it is assumed that nucleons making up the nucleus, couple their spins and magnetic moments to zero in pairs. Thus even A nuclei have zero spins and magnetic moments while odd A nuclei have spins and magnetic moments due only to the last odd nucleon.

The predictions of the shell model are in good agreement with experment for a very large number of nuclei. However, as one proceeds to high A nuclei a more detailed model is often necessary. Thus we have a slightly more complex model - the collective model.

(2) Collective Model.

A system of particles held together by their mutual attractions can undergo collective oscillations. This suggests a modification to the shell model. Instead of regarding the nucleons in closed shells as composing an inert core, Bohr and Mottelson[8] assumed that this core might exhibit effects of collective motion of the nucleons with it. This motion can take the form of either a rotation or a vibration, which is coupled to the motion of the nucleons outside of the closed shell.

In general this coupling is very complex, making the equations involved extremely difficult to solve. The coupling, however, takes a simplar form for nuclear configurations with closed or very nearly closed natron and

proton shells or for configurations far removed from closed shells. For these cases the motion of the nucleons outside of the last closed shell and the collective motion of the core can be considered separately. Thus, the excited states of these nuclei can be identified with either particle excitation or a collective excitation.

Several methods may be used to distinguish experimentally, the particle states from the collective states. One method employs the coulomb excitation[9] nuclear reaction. That is the nucleus is excited through an interaction between its own coulomb field and that of a closely passing bombarding particle. Only collective states are excited in this manner. Therefore, by measuring the energies of the gamma rays emitted by these excited nuclei, the energy levels associated with collective motions of the nucleons can be identified.

Nuclear Spectroscopy.

The foregoing discussion has shown that a number of properties of radioactive nuclei can be determined by a study of the radiations emitted during decay. In the field of nuclear spectroscopy we obtain from such measurements on nuclear radiations, information about the excited states of nuclei. This information together with that from other nuclear studies will, it is hoped, eventually lead to the formulation of a complete and satisfactory nuclear theory.

II. EXPERIMENTAL TECHNIQUES

A. Scintillation Spectrometer.

(1) General Description.

A block diagram of a single channel scintillation spectrometer is shown in figure 5. For gamma ray detection the detector consists of a sodium iodide crystal (activated with thallium) which is optically coupled to a photo multiplier tube. When a gamma ray is absorbed in the crystal a light scintillation is produced. The intensity of this scintillation is proportional to the energy of the absorbed gamma ray. Since the photomultiplier is a linear amplifying device the voltage pulse produced at the collector has an amplitude which is also proportional to the energy of the incident gamma ray. This pulse is further amplified with a linear amplifier and then fed into a pulse height analyzer. The pulse height analyzer registers an output pulse, which is recorded by the scaler, only if the pulse height falls within a predetermined voltage channel. The voltage about which the channel is centred may be varied from zero to one hundred volts. By scanning over the range of pulse heights from the amplifier one obtains peaks in the counting rate at voltages which are proportional to the energies of the absorbed photons. Figure 6 is an example of the type of spectrum obtained in this way.

(2) Detector.

Details of the construction of the scintillation detector are shown

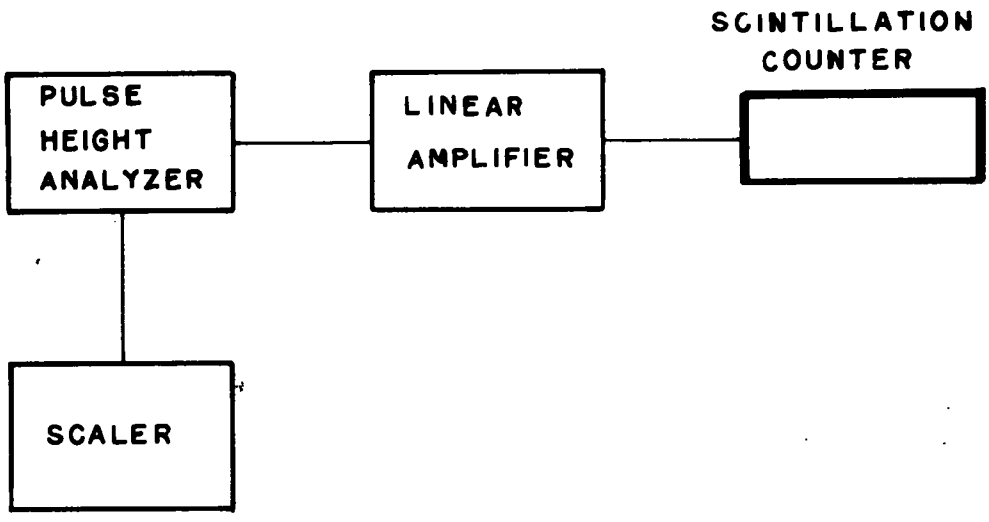

Scintillation Spectrometer

Figure 5

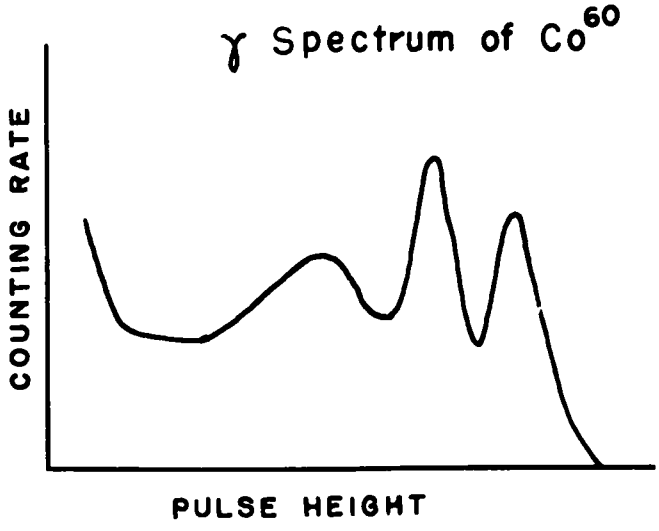

Figure 6

in figure 7. In order to keep the NaI crystal centered on the photo multiplier cathode, a fibre centering ring was placed on the photo multiplier. Optical coupling between the photo cathode and the crystal was achieved through a very thin layer of DC200 silicone oil. After the crystal was put in place and before it was wrapped with "scotch" electrical tape, Apeizon Q sealing compound was packed around the centering ring to prevent extraneous light from getting into the photo cathode. The crystal was held firmly against the photo multiplier with two pieces of electrical tape running parallel to the length of the tube and across the crystal. Finally the entire assembly was wrapped with electrical tape as an additional precaution against light leaks.

Voltage was applied to the photomultiplier dynodes from a voltage divider network consisting of nine 1 megohm resistors, one 2 megohm resistor, and one 10 K load resistor (see figure 8). The 2 megohm resistor was used between the cathode and first dynode, so that the voltage between these two elements would be twice that between other two successive dynodes.

The photo multiplier used in this detector was a DuMont 6292, which has a focussing electrode placed between the cathode and first dynode.

The manufacturer suggests that the potential on this electrode be adjusted to some value between that of the cathode and first dynode to optimize the photomultiplier response. It was found, however, that for the particular 6292 used, best performance was obtained when the focussing electrode was connected to the cathode.

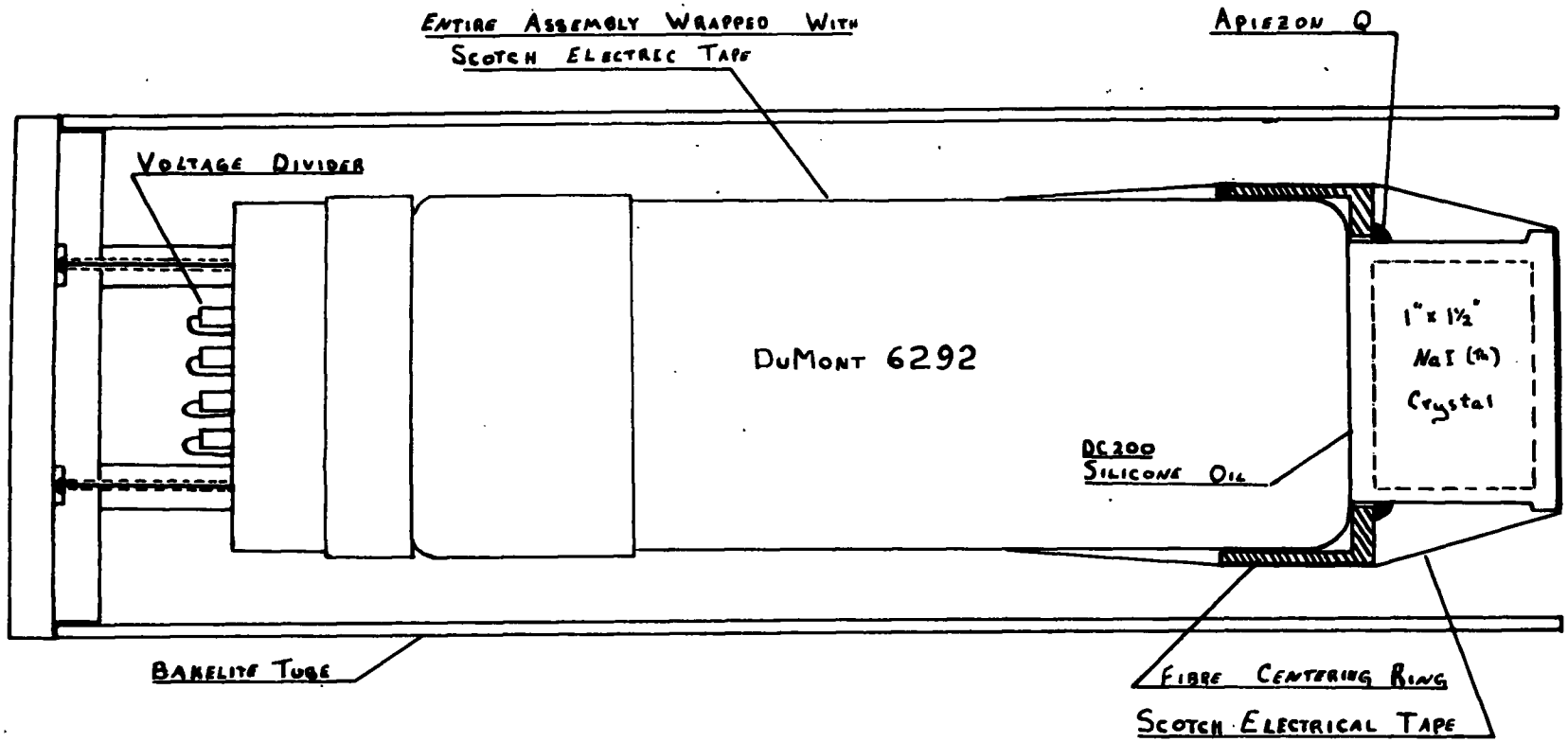
ENTIRE ASSEMBLY WRAPPED WITH
SCOTCH ELECTREC TAPE
APIEZON Q
VOLTAGE DIVIDER
DUMONT 6292
1" x 1½"
NaI (Tl)
Crystal
DC 200
SILICONE OIL
BAKELITE TUBE
FIBRE CENTERING RING
SCOTCH ELECTRICAL TAPE

FIGURE 7

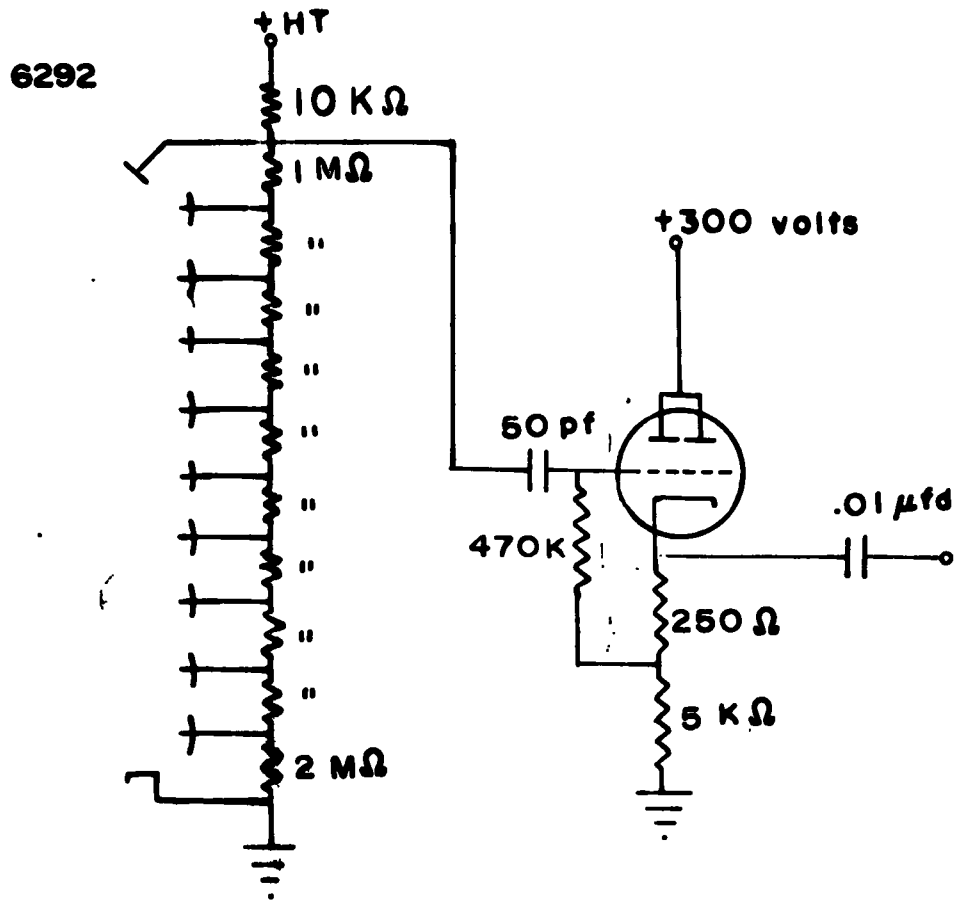

Detector Electronics

Figure 8

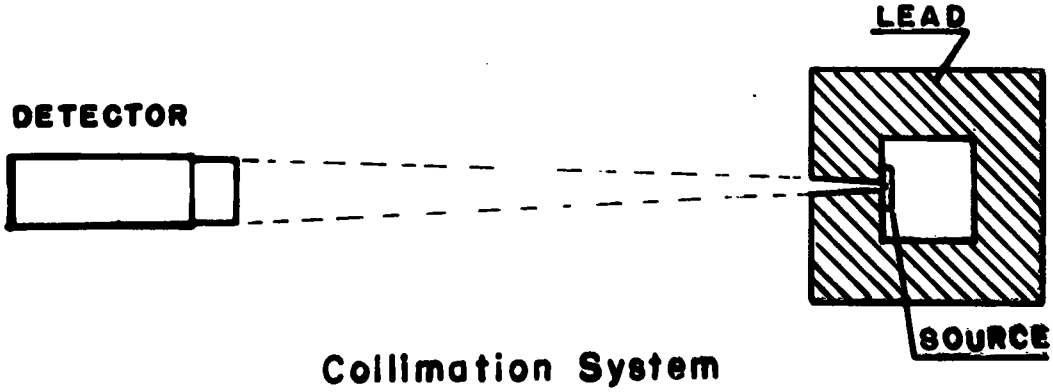

Collimation System

Figure 9

To energize the photomultiplier, 900 volts from a stabilized positive HT power supply was connected across the voltage divider network. The output pulses were then taken off at the collector through a 50 μμ fd condenser and fed into a cathode follower preamplifier (figure 8). The cathode follower circuit matched the output impedance of the photo multiplier to the 100 ohm characteristic impedance of the coaxial cables.

(3) Electronics.

The pulses from the cathode follower were amplified with an Atomic Instrument Co. Model 204B linear amplifier set at a maximum gain and at a 0.8 μsec risetime. The pulse height distribution at the output of the amplifier was then analyzed with an Atomic Instrument Co. Model 510 single channel pulse height analyzer. A scale of 64 scaler plus register was used to record the output from the pulse height analyzer.

(4) Source.

(i) Irradiation.

The Se^{75} source used in the present investigation, was prepared by irradiation of natural selenium with thermal neutrons, in the Chalk River pile. Other selenium activities produced are short lived, with the exception of Se^{79}, which has a very long half life ($\lesssim 6.5 \times 10^4$ years); a negligible amount of this activity is produced because of the relatively small capture crossection of Se^{78}.

(ii) Preparation for Spectroscopic Study.

For a study of its radiations the radioactive selenium was deposited as a small spot of red selenium on a thin LC 600 backing, which was supported by a one inch diameter aluminum ring. Preparation of the source in this manner is described in detail by McMahon[11].

(iii) Collimation.

The gamma ray detection efficiency of scintillation detectors is best for large source to crystal distances[12], i.e. for a parallel gamma ray beam incident on the crystal. However, placing the source at a large distance from the detector increases the probability that gamma rays will be scattered into the crystal through compton interactions in surrounding materials. To preserve the advantage of a large source to detector distance and at the same time eliminate scattering problems, collimation of gamma rays was employed.

The arrangement used to accomplish this is shown in figure 9.

(4) Measurement of The Gamma Ray Spectrum.

With the pulse height analyzer channel width set at one volt, the counting rates were measured for baseline settings spaced at one volt intervals, from 0 to 70 volts. Since the detection efficiency of the scintillation counters is very high one minute counts on each point gave a statistical accuracy of better than 1% on the peaks and 4% elsewhere.

B. Gamma-Gamma Coincidence Spectrometer.

(1) Description.

The high detection efficiency of scintillation counters makes them ideally suited as gamma ray detectors in coincidence counting experiments. In the present investigation, coincident gamma radiations were measured using the system outlined in the block diagram in figure 10.

Basically the apparatus consists of two scintillation spectrometers, like the one described in [A], plus an Atomic Instrument Co. Model 502A coincidence analyzer. This instrument has four coincidence channels, only two of which were used in the present spectrometer. Each channel has an adjustable resolving time from 0.25 micro seconds to 2.0 micro seconds. For reasons which will be explained later the total resolving time (i.e. the sum of the resolving times of the two channels used) was set at approximately one micro second.

In order to get a high coincidence counting rate, the two detectors were placed very close to the source. For most measurements, source to crystal distances of one centimeter were used, with detectors on opposite sides of the source.

The Se^{75} source used was prepared as a small spot on a rubber hydrobromide backing. This backing was supported on a two inch diameter ring made of aluminum wire. The source was supported in this manner to minimize the possibility of Compton scattering in the source holder.

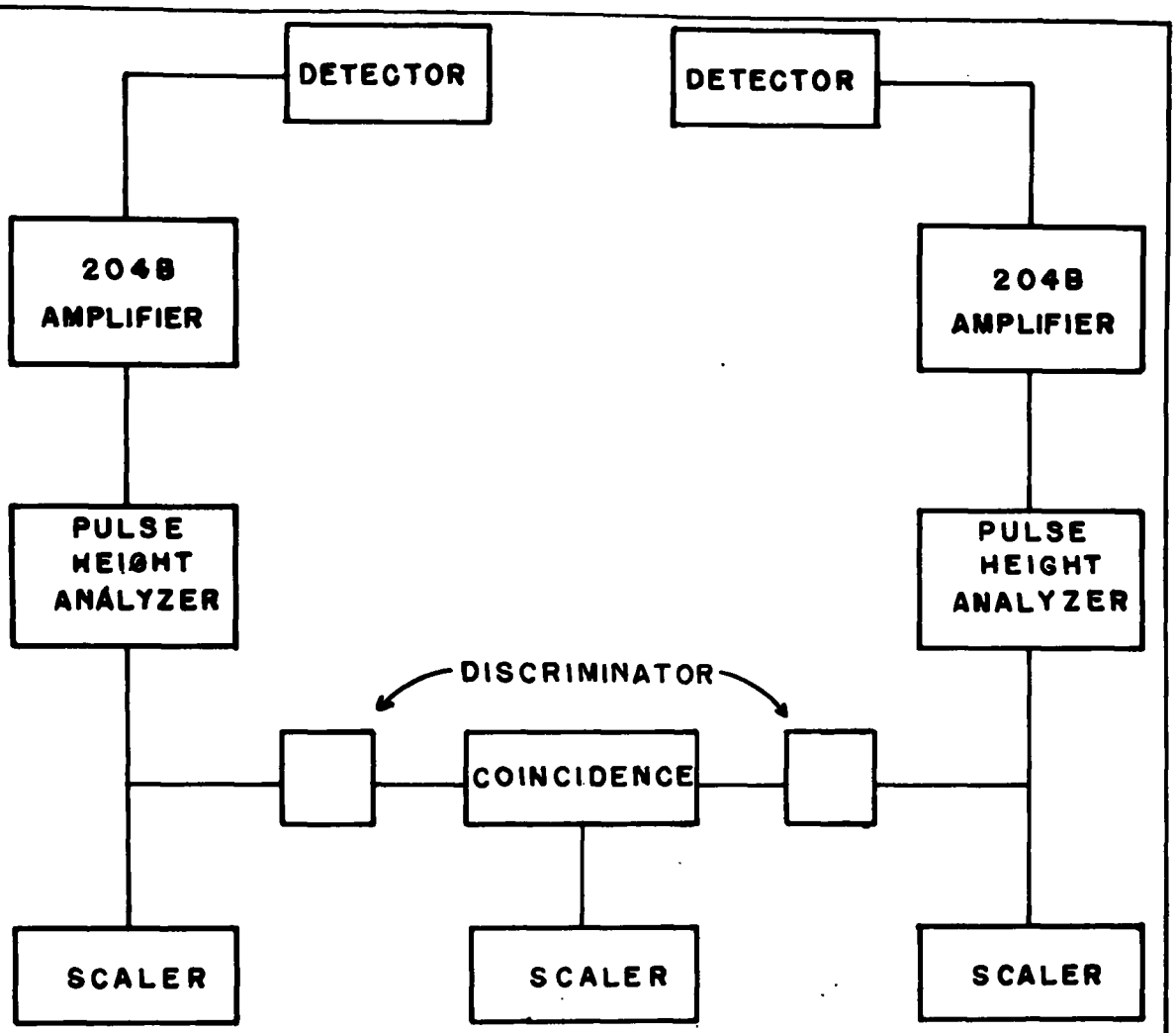

$\gamma\gamma$ COINCIDENCE SPECTROMETER

Figure 10

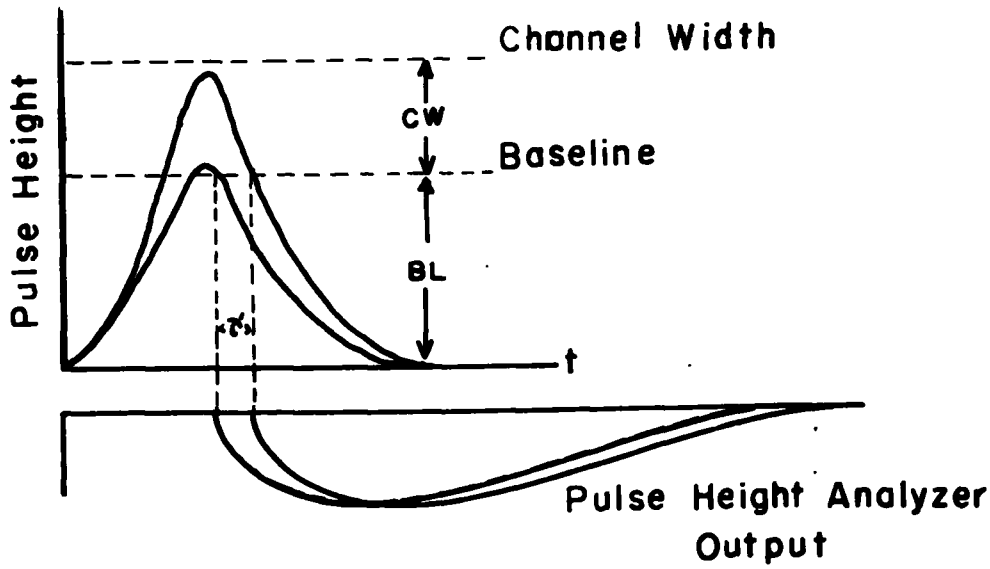

Figure 11

(2) Resolving Time.

The use of the Model 510 pulse height analyzers in the coincidence spectrometer outlined in figure 10 places certain restrictions on the coincidence resolving time that can be used. This results from the fact that the output pulse from the analyzer occurs when the triggering pulse recrosses the baseline discrimination level. That is, the pulse at the output is delayed with respect to the input by an amount equal to the width of the pulse above the baseline discrimation level. A fixed delay due to the electronics is not serious, since compensation for this can be made, however, the above mentioned delay is in effect a variable one, depending upon the pulse height. This effect is illustrated in figure 11.

Pulses "a" and "b" represent the two extreme pulses that will be recorded by the pulse height analyzer for general baseline setting B.L. and a channel width C.W. Pulse "a" produces an output pulse a time τ' later than pulse "b". The magnitude of τ' is governed by the channel width and the slope of the trailing edge of the pulse. The shape of the pulse is determined by the amplifier circuitry and is not easily changed. Therefore, to keep τ' small a narrow channel width is indicated. This was always set at less than 2 volts, which then gave a τ' of 0.5 micro seconds. This value represents the minimum resolving time that the coincidence analyzer can have. A resolving time of 1 micro second was chosen so that allowance could also be made for possible additional variations in delay due to slight drifting in the discrimination levels at the inputs to the coincidence analyzer. The dependence of the delay on the discrimation level results from the long

rise time of the pulse height analyzer output pulse.

To measure the coincidence resolving time, pulses from a scintillation detector were fed into one amplifier while the output from a pulser was used as the input to the other amplifier. With this arrangement the pulses registered by the coincidence analyzer must be due only to chance. The chance coincidence rate is related to the resolving time by,

$$N_{ch} = N_1 N_2 \tau \qquad (13)$$

Where, N_1, N_2 are the counting rates in each channel of the coincidence analyzer. Hence τ can be calculated.

(3) Measurement of Gamma-Gamma Coincidences.

With one pulse height analyzer chanelled on a gamma ray peak the coincidence counting rate was recorded as the other pulse height analyzer was scanned over the entire spectrum. Peaks occur in the coincidence spectrum corresponding to the gamma rays coincident with the one in the fixed channel.

The two largest peaks in the scintillation gamma ray spectrum of Se^{75} are actually composite peaks; one corresponding to a 121 and a 137 kev gamma ray and the other to a 265 and a 280 kev gamma ray. Coincidences with these gamma rays were measured by setting the fixed channel first on the high side of the peak, so as to accept more of the high energy component and later on the low side to accept more of the low energy component.

The single channel counting rates were also measured so that the chance coincidence rate could be calculated using equation (13) the calculated chance rate was substracted from the observed coincidence rate, to obtain the significant coincidence rate.

C. Beta-Gamma Coincidence Spectrometer.

The coincidence measurements just described are limited by the poor resolution of the scintillation counters. For this reason it was decided to attempt to measure conversion electron - gamma coincidences using a magnetic and a scintillation spectrometer. In this way we utilize the high resolution of the magnetic spectrometer and the high transmission of the scintillation spectrometer. A block diagram of the $\beta - \gamma$ coincidence spectrometer is shown in figure 12.

(1) Magnetic Spectrometer.

A modified thin lens spectrometer, described in detail by Milley[13] was used as the conversion electron detection system. This spectrometer differs from the conventional thin lens spectrometer in two respects; 1) the source and detector are not equidistant from the center of the magnet. 2) Ring focus detection is used instead of the axial detection in conventional spectrometers. These modifications improve the transmission by a factor 9 while not altering the resolution.

Ring focus detection is achieved with a ring of anthracene crystals

coupled to a "conical" light pipe with silicone oil. The light pipe transmits the scintillations from the ring, which is 5 inches in diameter onto the $1\frac{1}{2}$ inch diameter photo cathode of the photo multiplier tube. Milley used a DuMont 6292 photo multiplier, in the present work, however, this was changed to a 14 stage EMI 6262 tube.

This change was made in an effort to get signal pulses from the amplifier with amplitudes sufficiently high to allow the use of a discrimination level that was above the level of most electrical interference, (caused primarily flourescent lights in the building).

Optical coupling between the photo cathode and the light pipe is secured by coating the end of the photo multiplier with silicone oil and then pressing it firmly against the light pipe.

Magnetic shielding is provided by having the photo multiplier inside a mild steel tube which is fastened to the end of the spectrometer.

Pulses from the photo multiplier are fed through a cathode follower preamplifier to a Model 204B amplifier (set at a 0.2 μ sec. risetime). The output from the amplifier is recorded with a scaler plus register.

To provide a necessary time delay adjustment when the spectrometer is used for beta-gamma coincidences, a variable delay line is placed at the output of the amplifier.

The measurement of beta spectra with the magnetic spectrometer is accomplished by varying the current through the coil in steps, and recording the corresponding counting rates. For each current setting the magnetic

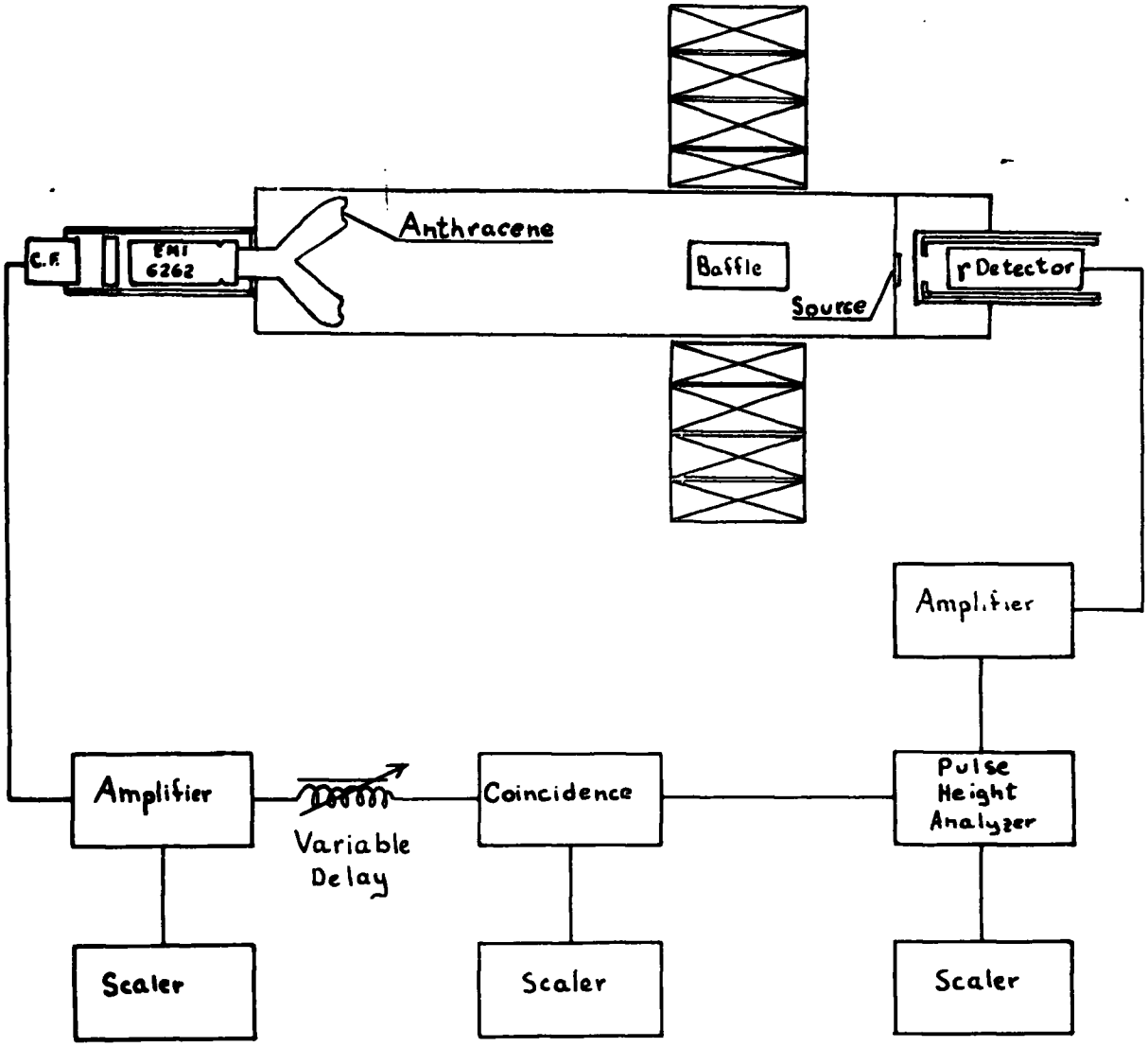

Figure 12 $\beta-\gamma$ COINCIDENCE SPECTROMETER

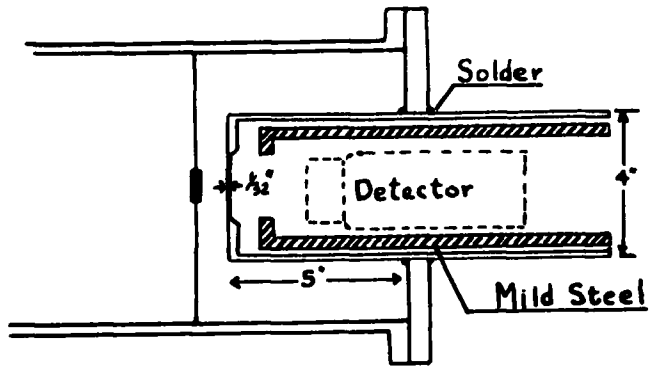

Figure 13 ENDPLATE MODIFICATION

field produced focusses beta particles with a particular momentum, on the anthracene crystals. From the above procedure therefore, one can get the momentum distribution of the emitted beta particles.

In order to allow the gamma ray detector to be placed near the source for beta-gamma coincidence measurements, the end plate at the source end of the magnetic spectrometer had to be modified. This modification is illustrated in figure 13. The mild steel tubing shown is this figure provides magnetic shielding for the photo multiplier.

(2) Preliminary Tests and Adjustments.

(i) Single Channel Spectra.

A trial conversion electron spectrum of Se^{75} was measured to determine the effect, if any, of the brass and iron placed near the source as a result of the modification described above. The results of this test showed no significant change in the shape of the conversion spectrum, nor was there any evidence of hysterisis effects due to the magnetic shield.

The gamma ray spectrum measured with the scintillation spectrometer does show some distortion due to Compton scattering from either the surrounding brass or iron. Since the photo electron peaks were still quite prominent, the distortion was not considered to be serious.

(3) Delay Time Matching.

To compensate for the time delay introduced by the pulse height analyzer, a variable delay line was inserted in the magnetic spectrometer

circuit. The amount of delay required was found by feeding into both 204B amplifiers, the output from the pulser. The delay was then varied until all of the pulses were counted by the coincidence circuit.

(4) Measurement of Beta-Gamma Coincidences.

Measurement of conversion electron-gamma coincidences in the Se^{75} spectrum were made both by fixing the magnetic spectrometer on a peak and scanning with the scintillation spectrometer and visa versa. Because of the relatively low transmission of the magnetic spectrometer ($\sim 2.5\%$) the coincidence counting rate was very low. As a result counting times as long as 100 minutes on a point were often necessary to obtain statistically significant results.

D. Angular Correlation.

Some preliminary gamma-gamma angular correlation experiments were performed in an attempt to gain further information about energy level spins and transition multipolarities. The 137 - 265 kev cascade was chosen as the one to be studied. This experiment yielded a correlation function with negative anisotropy of 5.5 %. Interpretation of the results is, however, not possible at this time because insufficient information has been obtained to allow a correction to be made for the effect of the unavoidable detection of the 121 - 280 kev cascade. Even when this correction can be made, interpretation of the angular correlation results will be difficult because conversion coefficients indicate that both the 137 and the 265 kev gamma rays are probably mixed E2 + M1.

III. EXPERIMENTAL RESULTS ON THE DECAY OF Se^{75}

1. Outline of Previous Work.

Se^{75} (127 days) decays by electron capture to one of several excited states of As^{75}. The results of a number of investigations of this decay have been published. Good agreement exists on the gamma ray energies of 66, 97, 121, 137, 199, 265, 280, 305 and 402 kev.[11,14,15,16,17]. Cork et al[15] have measured the conversion electron spectrum using a π spectrometer and photographic detection. They report conversion lines corresponding to transition energies of 24.7, 66.2, 80.8, 96.8, 121.2, 136.2, 198.8, 265.2, 280.1, 304.0, 401.9 kev. On the basis of these energy measurements a decay scheme is proposed. Jensen et al[16] have also measured the conversion electron spectrum. They did not observe any evidence for the 24.7 or the 80.8 kev transitions but did find a fairly intense 77 kev transition. From the conversion electron studies and some preliminary coincidence measurements they propose a decay scheme which differs from Cork's because of the omission of the 24.7 and the 80.8 kev transitions and the inclusion instead of the 77 kev transition. Temmer and Heydenburg[18] have induced by coulomb excitation the 66, 199 and 283 kev transitions. These results are consistent only with Cork's decay scheme.

Crystal summing techniques employed by Lu, Kelly and Weidenback show that the highest level in As^{75} resulting from decay of Se^{75} is at

402 kev.

The most recent and also the most extensive investigation of the Se^{75} decay scheme has been carried out by Schardt and Welker[17].

They have measured gamma ray energies, internal conversion coefficients, and relative transition intensities. In addition they have performed gamma-gamma coincidence and angular correlation measurements. They also studied the decay of Ge^{75}, which decays by beta emission to As^{75}. From these measurements a level scheme for As^{75} is proposed and plausible spin and parity assignments are discussed.

2. Results of the Present Investigation.

(i) Relative Transition Intensities.

The relative gamma ray intensities are obtained from the spectrum measured with the scintillation spectrometer (figure 14). The areas under the photo-peak, corrected for the photo-peak efficiency (Appendix I) was taken as a measure of the gamma ray intensity. Compton distributions associated with the (121 - 137) and (265 - 280) kev peaks were calculated using Compton scattering cross sections given by Davisson and Evans[20]. These were subtracted from the spectrum before the areas of the 66 kev and 97 kev peaks were measured. For these two transitions a correction was also made for the escape of the iodine X ray (Appendix II). The relative gamma ray intensities are summarized in table 4 column 2. Column 3 summarizes the gamma ray intensities obtained by Schardt and Welker[17] from a photo electron spectrum using a lead radiator and a thin lens spectrometer. The 305 and 280

Transition Energy kev	Scintillation γ Intensity	Schardt & Welker[11] Photoelectron Intensity	Final γ Intensity	McMahon[11] Conversion Intensity	K/L	Conversion Coefficient	Transition Intensity	Multipole Assignment
402	0.16		0.23	0.026K		2.15(-3)*	5.66%	M1
305		0.02	0.02	0.13K		1.28(-1)	0.57%	E2?
280	1.00	0.457	0.46	0.5K		2.15(-2)	11.55%	E2
265		1.00	1.00	1.00K		1.95(-2)	25.0 %	E2+M1
199	0.06		0.087	0.057K		1.23(-2)	2.62%	M1
136	1.15	1.00	1.29	3.78K	11.4	5.85(-2)	33.5 %	E2+M1
121		0.301	0.39	1.57K		8.10(-2)	11.1 %	M1
97	0.14	0.052	0.20	7.80K	6.8	7.70(-1)	8.6%	E2
81	Not observed							
66	0.048		0.07	0.33K	~ 7	9.25(-2)	1.87%	E2+M1
25	< 0.02		< 0.029					

* (-3) $\equiv 10^{-3}$

Conversion Coefficients and Transition Intensities for As^{75}

TABLE 4

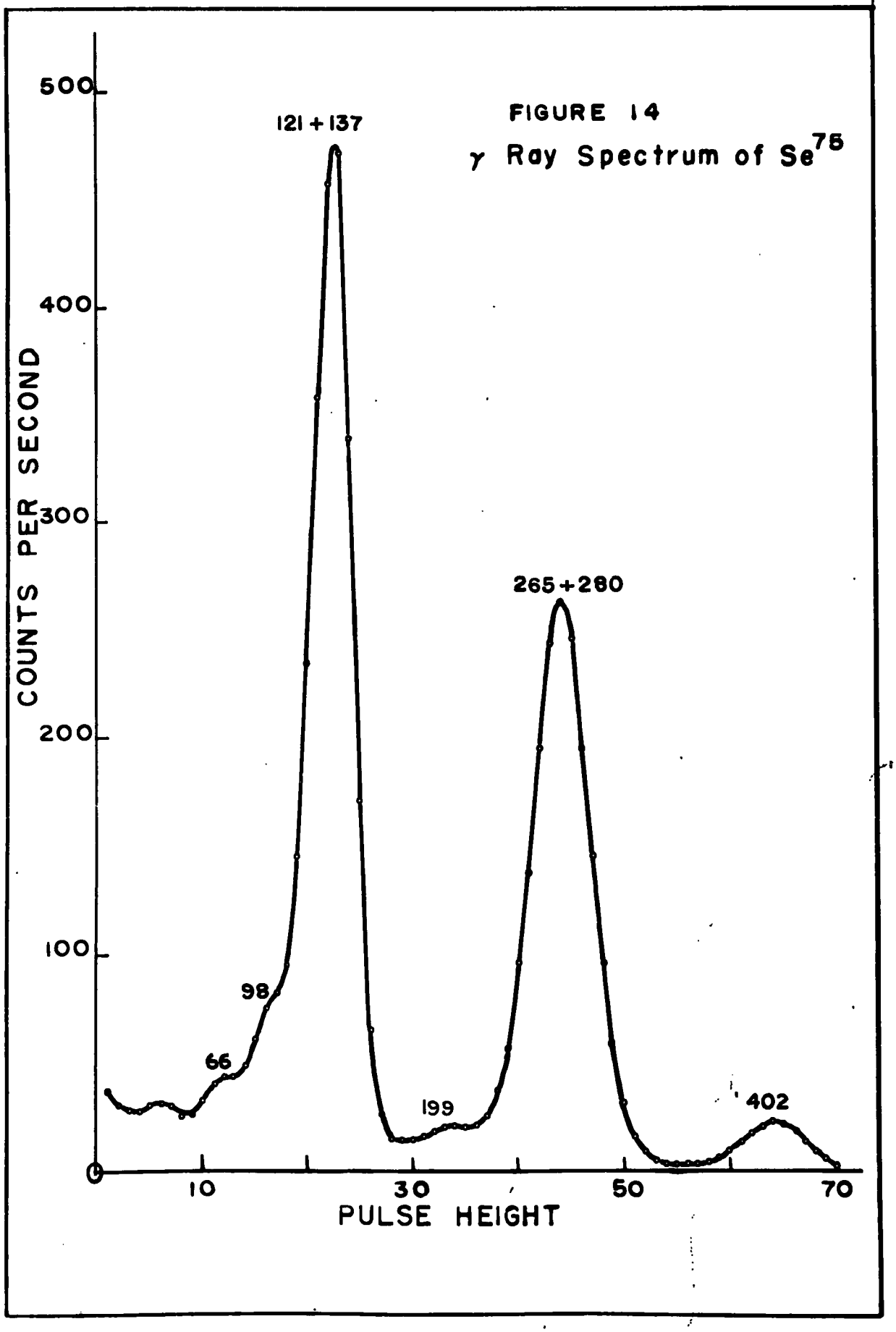
FIGURE 14
γ Ray Spectrum of Se75
COUNTS PER SECOND
500
400
300
200
100
0
121 + 137
265 + 280
98
66
199
402
10
30
50
70
PULSE HEIGHT

kev gamma ray intensities are expressed relative to that of the 265 kev gamma ray; while the intensities of the 121 and 97 kev gamma rays are given relative to that of the 137 kev gamma ray.

The final relative intensities are arrived at by dividing the intensities of the (265, 280) and (121, 137) composite peaks according to the relative intensities of the two gamma rays in each peak. Column 4 of Table 4 lists the final gamma ray intensities, normalized to that of the 265 kev gamma ray.

The conversion electron intensities listed in column 5 and the K/L ratios in column 6 were measured by McMahon[11] using a thin lens spectrometer set at 2.5% resolution. Relative conversion coefficients are obtained by dividing the conversion intensities by the corresponding gamma ray intensities. With the identification of the 97 kev transition as being E2, (reasons for this assignment to be discussed later) the relative conversion coefficients can be converted to absolute values.

Multiplying the gamma ray intensity by the corresponding conversion coefficient and adding the product to the gamma ray intensity gives the total transition intensity which is listed in column 8 of Table 4.

(ii) Identification of Gamma-Gamma Cascades.

The existence of various gamma-gamma cascades was established through the coincidence measurements. A typical spectrum obtained with the scintillation coincidence spectrometer is shown in figure 15.

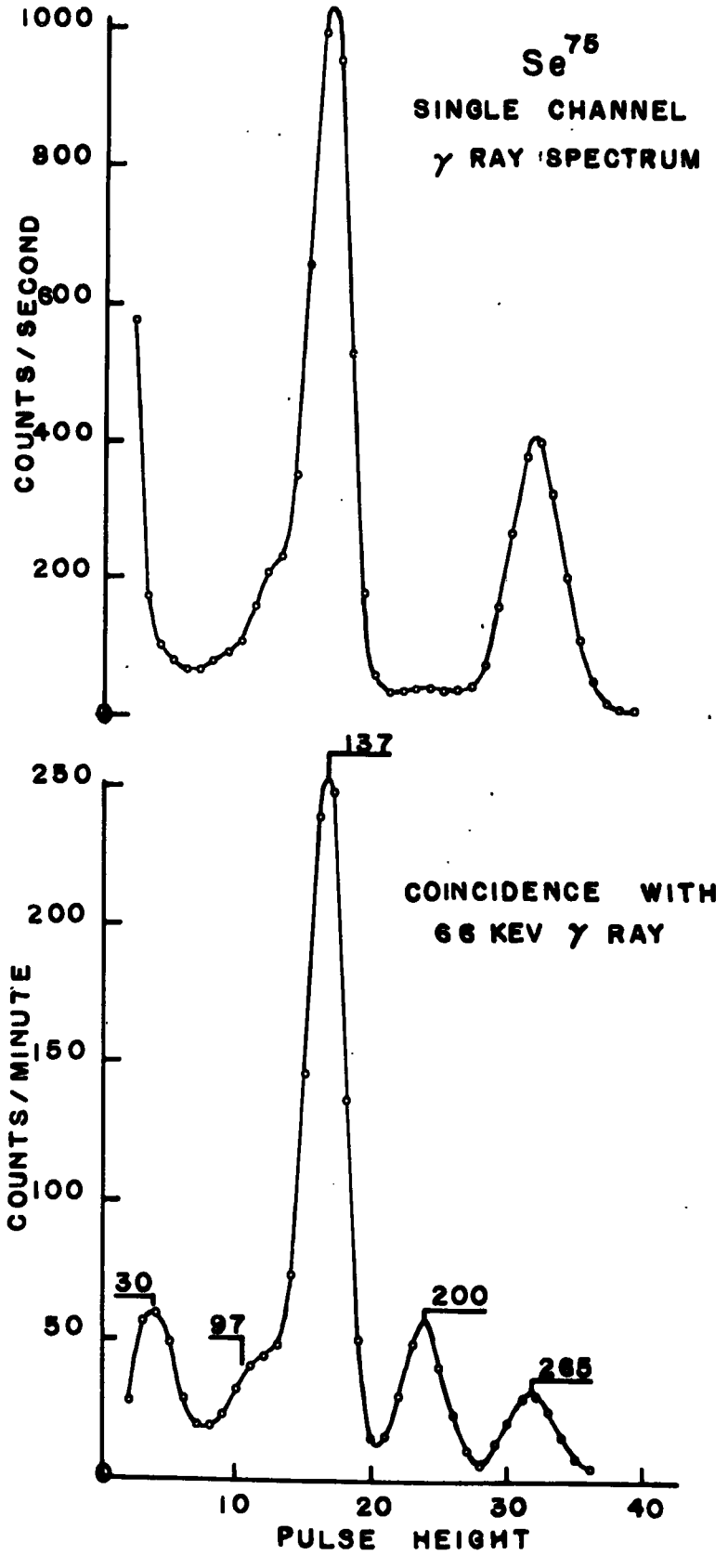
1000
800
600
400
200
COUNTS / SECOND
Se^{75}
SINGLE CHANNEL
γ RAY SPECTRUM
250
200
150
100
50
COUNTS / MINUTE
137
COINCIDENCE WITH
66 KEV γ RAY
30
97
200
265
10
20
30
40
PULSE HEIGHT

Figure 15

Considerable care must be taken in interpreting the coincidence spectra because in general, pulses due to other than the gamma ray of interest fall into the pulse selection channels. For example, when the fixed channel is set to accept pulses due to the 66 kev gamma ray, it will accept an almost equal number of pulses due to the 97 and 137 kev gamma rays and the Compton distribution associated with the (265, 280) kev peak. The presence of the 265 and 98 kev peaks in figure 15 can be explained by detection of these "extraneous" pulses. The possibility of scattering of radiation from one detector to the other must also be considered in certain cases. It is believed that such a scattering process accounts for part of the observed 137 kev coincidence peak when the fixed channel is set to accept 137 kev pulses. (A small coincidence peak at 137 kev would be expected, since included in the fixed channel there will be some of the Compton distribution association with the (265, 280) kev photo-peak and these are in cascade). Related to crystal scattering is the detection in one crystal of the iodine X-ray which escapes from the other. The peak at 30 kev in figure 15 can be attributed to this effect.

The results of the gamma-gamma coincidence measurements are summarized in Table 5. As can be seen coincidences between the composites peaks of (97, 121, 137) and (265, 280) kev are fairly easily established. To obtain more specific information about the cascades involving these gamma rays, conversion electron-gamma coincidences were measured. The higher resolution of the magnetic spectrometer allowed coincidences with the 97, 121, and 137

TABLE 5

Se^{75} Gamma-Gamma Coincidences

Selected Event (kev)	Coincidences	Comments
402	None	
(265, 280)	(121, 137)c	There are no coincidences above 137 kev.
200	66	
	137	
137	66	
	(265, 280)c	
98 (favored) 137, 121 66		No coincidence could be established because of interference from other gamma rays
280 303	121	
	98	
66	(121, 137)	
	200	

Note: c - composite peak.

kev conversion electron to be measured separately.

Figure 16 shows a typical coincidence spectrum obtained in this manner. The coincidence peak at 121 and 137 kev are caused by detection of Compton scattered 265 and 280 kev gamma rays in the scintillation counter. Table 6 summarizes the results of the conversion electron-gamma coincidence measurements.

Multipole Assignment to 97 kev. Transition.

Identification of the 97 kev transition as being E2 is based on the measured K/L ratio and on the fact that consistent multipole assignments to other transitions can be made on the basis of conversion coefficients, calculated as a result of this identification.

The K/L ratio as measured by McMahon[11] is 6.8. According to the empirical K/L ratio ratio curves of Goldhaber and Sunyar this would mean that the 97 kev. transition is either E2, M2 or M3. If it were M3 a metastable state with a life time of 3.5 minutes would be expected[21]. Jensen et al[16] searched for such a state with negative results. The choice is, therefore, narrowed to E2 or M2. E2 is preferred because the M2 transition probability is too small to explain competition with other gamma rays which proceed from the 402 kev. level. Schardt and Welker have measured the conversion coefficient of the 402 kev. transition relative to the conversion coefficient ($\alpha = 0.118$) of the 661 kev. Cs^{137} transition. Their value of (2.4×10^{-3}) is in excellent agreement with the value (2.2×10^{-3}) obtained from the present results on the assumption of a 97 kev. E2 transition.

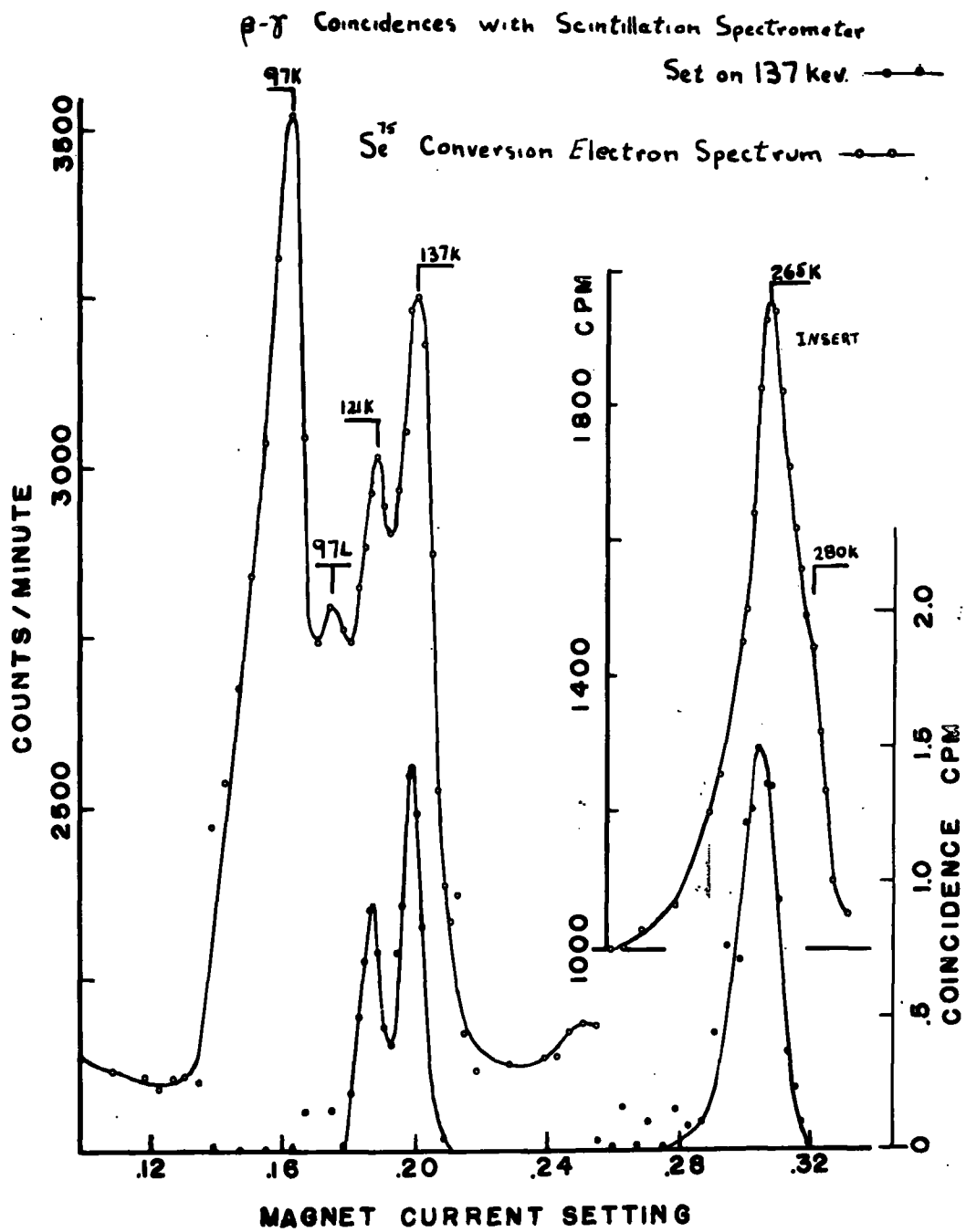
β-γ Coincidences with Scintillation Spectrometer
Set on 137 kev.
Se⁷⁵ Conversion Electron Spectrum
97K
137K
121K
97L
265K
280K
INSERT
COUNTS / MINUTE
3500
3000
2500
1800 CPM
1400
1000
2.0
1.5
1.0
.5
0
COINCIDENCE CPM
.12
.16
.20
.24
.28
.32
MAGNET CURRENT SETTING

Figure 16

TABLE 6

Conversion Electron - Gamma Coincidences:

Selected Event	Coincidence
97 kev.Conversion Electron	(265, 280)c Gamma
137 kev.Conversion Electron	(265, 280)c Gamma
121 kev.Conversion Electron	(265, 280)c Gamma
137 kev. Gamma	265 kev. Conversion Electron
280 kev. Gamma	121 kev.Conversion Electron

Note: c - composite peak.

3. Discussion of the Decay Scheme of As^{75}.

The energy level sequence with spin and parity assignments, as well as the multipolarities of the transitions in As^{75} are made on the basis of previously published investigations of this decay, in addition to conversion coefficients, intensity measurements and coincidence measurements of the present work.

The level scheme shown in figure 17 is identical to that proposed by Cork et al[15] and differs from Schardt and Welkers[17] only in the omission of the 477 and 628 kev. levels, which are excited through beta decay of Ge^{75}. All of the observed coincidence cascades are accounted for by this decay scheme. It is, however, not possible to determine directly the order of emission of the 121 - 280 kev. gamma rays, and the 97 - 305 kev. gamma rays. It would be possible therefore to replace the levels at 280 and 305 kev. by ones at 121 and 97 kev. The latter scheme is not very likely though, since neither the 97 nor the 121 kev. transition is excited by coulomb excitation. To be ground state transitions and not be excited by coulomb excitation, the 121 and 97 kev. transitions would have to be pure magnetic multipoles, which does not agree with conversion coefficient data.

A level is placed at 200 kev. rather than at 66 kev. on the basis of Schardt and Welker's[17] study of the beta decay of Ge^{75}. They observe a beta decay to a 628 kev. level in As^{75} and a 427 gamma ray (among others) in coincidence with it. Such a gamma transition can be accounted for, if there is a level at 200 kev.

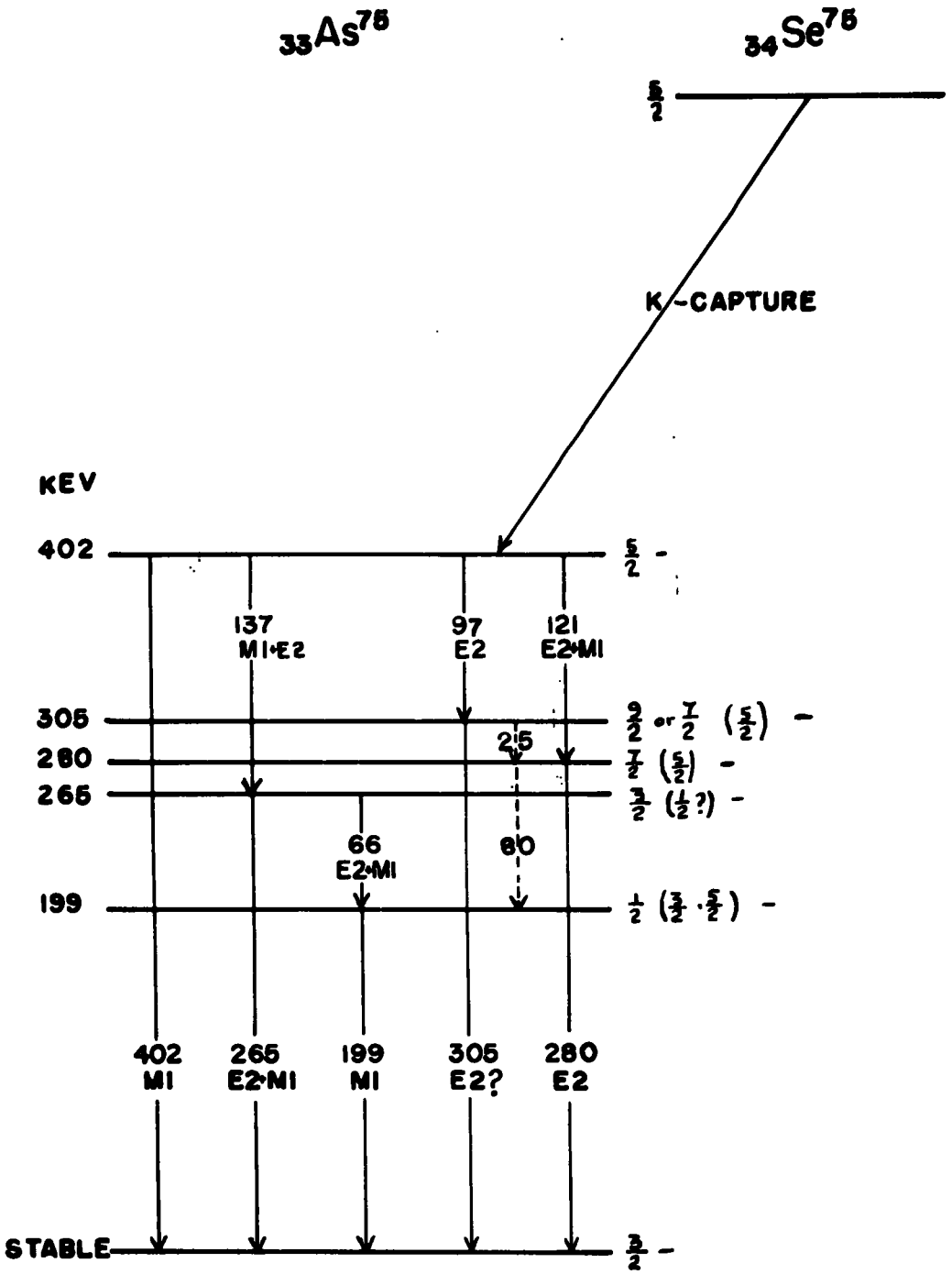

DECAY SCHEME OF SELENIUM 75

Figure 17

The spin of Se^{75} has been measured using microwave spectroscopy techniques[22] and found to be 5/2. The shell model predicts a spin of either $\frac{1}{2}$ or 9/2.

Trail and Johnson[23] have measured the threshold energy of the reaction,

$$As^{75} (p, n) Se^{75}$$

and obtained 1.674 ± 0.005 Mev. The energy difference between the ground states of As^{75} and Se^{75} calculated from this threshold energy is 900 kev. From this information the log ft values for decays to the various levels can be calculated using the graphs of Moszkowski[3]. In particular the log ft value for the decay to the 402 kev. level is 6.2, which indicates that this decay is probably allowed. Hence the 402 level could have spins of 7/2, 5/2 or 3/2. The conversion coefficient for the 402 kev transition agrees very well with the theoretical value for an M1 transition. Therefore, since the spin of the ground state of As^{75} is 3/2 (-)[24], the 7/2 spin choice for the 402 kev. level is eliminated. Spins of 5/2 and 3/2 remain as possibilities with the 5/2 being more likely because of the M1 ground state transition. This choice is also indicated by the studies[17] of the beta decay of Ge^{75} to As^{75}. The ground state of Ge^{75} is very likely 1/2 and thefore if the 402 kev. level of As^{75} were 3/2, one would expect a beta decay to this level. Since no such decay is observed the argument in favour of the 5/2(-) choice is strengthened.

The 97 kev. transition was identified as E2, which means that the

305 kev. level can have a spin of 9/2, 7/2, 5/2, 3/2 or 1/2.

From the conversion coefficient data, the 280 kev. transition was identified as E2. Therefore the possible spins of the 280 kev. level are 7/2, 5/2, 3/2 or 1/2.

The conversion coefficient for the 265 kev. transition indicates that it is rather pure E2, but some M1 mixing would be consistent with the results. With an E2 + M1 identification for this transition the possible spins of the 265 kev. level are 5/2, 3/2, or1/2. The log ft value for beta decay from Ge^{75} to the 265 kev. level is 5.6^{17} (i.e. an allowed beta decay). Hence the spin of the 265 level is either 3/2 or 1/2. The value of 1/2 would be preferred since the 265 dev. transition is an E2 type and goes to the 3/2 ground state. This choice would require the multipolarity of the 137 kev. transition to be at least E2. However, the measured conversion coefficient for the 137 kev. transition is near the theoretical value for M1 but a factor 10 smaller than the theoretical value for an E2 transition. Tentatively, therefore, a spin of 3/2 is assigned to the 265 kev. level.

The 200 kev. transition has a measured conversion coefficient which agrees very well with an M1 assignment. Thus the possible spins for the 200 kev. level are 5/2, 3/2 or 1/2. Unfortunately, the measured conversion coefficient for the 66 kev. transition isnot very accurate. It appears to be closest to the theoretical value for M1 which would be consistent with spin assignments of the 265 and 200 kev. levels.

Looking at the 305 kev. transition, it is seen that it could be M3, E2 or M1 with M3 more likely on the basis of spin change alone. This assignment agrees, within experimental error, with the measured conversion coefficient. Again, however, this conversion coefficient is not known too accurately because of the low intensity of the 305 kev. transition. An assignment of M3 would mean that this transition would have an expected lifetime of 0.08 seconds.[21]

The existence of such an isomeric state is not expected. Feenberg and Hammack[26] and Nordheim[27] have pointed out that "islands of isomerism" exist for odd A nuclei with $39 \leq$ (odd Nor Z) ≤ 49 and for $63 \leq$ (odd N or Z) ≤ 81. As^{75} with 33 protons and even N does not fit into either one of these islands. Therefore, in the absence of definite evidence for the existance of an isomeric state, the 305 kev. transition has tentatively been labelled E2. It might, however, be noted here that identifying the 305 level as an isomeric state would explain the pronounced 97 kev. peak in the summed spectrum[19].

The 80 kev. transition was not detected in the present investigation but is reported to be weak.[17] This would be expected from the spin assignment of the 280 and 200 kev. levels.

Conclusion.

The results of this investigation are summarized by the decay scheme in figure 17. The sequence of energy levels in As^{75} seems to be fairly well established. The spin assignments to the various levels are made on the basis of foregoing arguments, and differ in some respects from those proposed by Schardt and Welker.[17] In cases where unambiguous assignments could not be made, the most probable spin is indicated first, with the less probable ones enclosed in parenthesis. It is expected that more accurate measurements on the low intensity transitions will provide the necessary information to remove these ambiguities.

APPENDIX 1

Gamma Ray Detection Efficiency of a NaI (Th) Crystal

Gamma rays that are incident on a scintillation crystal may be absorbed through one of three processes; they are, photo electric effect, Compton effect and pair production. The latter is possible only if the gamma ray energy is greater than 1.02 mev. Since the present work deals only with gamma rays having energies less than 400 kev., absorption by pair production need not be considered here. In a photo electric interaction the entire gamma ray energy is transferred to a bound electron. Thus the intensity of the scintillation produced is proportional to the gamma ray energy (provided that the X-ray produced is also absorbed). The Compton effect on the other hand results in only part of the original gamma ray energy being transferred to an electron, the remainder appearing as a scattered photon.

Escape of the scattered photon from the crystal, then results in a scintillation, the intensity of which is proportional to the energy transferred to the electron. Since this energy is not fixed, but depends upon the scattering angle, Compton processes result in a rather broad pulse height distribution, unlike the sharp peaks produced by photo electric processes. The scattered photon may however undergo further interactions in the crystal and ultimately the entire gamma ray energy may be absorbed in the crystal. This multiple process results in the same pulse height as

if the gamma ray had been absorbed through a photo electric process directly. Such a process is quite desirable since it increases the intensity of the photo electric peak, and as we shall see below, only this peak is of interest in calculating relative intensities of gamma rays.

The photo electric peaks have a shape which is indist inguishable from a Gaussian curve. It is therefore a fairly simple matter to obtain the areas under these peaks. This area is proportional to the number of pulses in the photo-peak, and when corrected for photo-peak detection efficiency one has a measure of the relative gamma ray intensity.

Using total absorption cross sections for NaI , Bell[12] has prepared a set of curves, for a number of source to crystal distances, giving the total detection efficiency as a function of gamma ray energy for a 1" x 1½" crystal. A variation in efficiency with source position results from crystal edge penetration effects, i.e. for moderate source distances the thickness of crystal seen by the gamma ray varies considerably with different angles of emission. By multiplying the total efficiency factor obtained from these graphs by the fraction of pulses that are in the photo-peak, one gets the corresponding photo-peak efficiency. The peak to total ratio as a function of energy has been measured by Bell[28] for the 1" x 1½" crystal. A measured rather than a calculated ratio must be used because the amount by which the intensity of the photo-peak is increased by multiple absorption processes is difficult to calculate.

To summarize then, relative gamma ray intensities are obtained from a scintillation spectrum as follows:

1) Gaussian curves are fitted to the photo electric peak and the area under the peak determined.

2) From Bell's curves the appropriate total efficiency is determined and multiplied by the peak to total ratio.

3) The photo-peak area is divided by the photo-peak efficiency (determined in 2) to give a measure of the relative gamma ray intensity.

APPENDIX II

Correction for the Escape of the Iodine X-ray

Low energy gamma rays are absorbed through a photo electric process very near the surface of the crystal, consequently the I X-ray so produced has a good chance to escape from the crystal. This then results in an escape peak at 30 kev. below the main photo electric peak. The ratio of the number of X-rays that leave the crystal to the number of gamma rays incident has been measured[29] as a function of gamma ray energy.

In the case of the Se^{75} spectrum the escape peaks of the (121, 137) kev. gamma rays fall very near to the 97 kev. photo-peak, and the escape peak of the 97 kev. gamma ray falls on the 66 kev. peak. Because of the presence of the escape peaks the intensities of the 66 and 97 kev. gamma rays in measured using the following procedure: Gaussian curves are fitted to the spectrum at (121, 137), 97 and 66 kev. The half width of the Gaussians at 97 and 66 kev. are determined by using the fact that the resolution of the scintillation spectrometer is inversely proportioned to $\sqrt{E}$, where E is the gamm ray energy. The area of the (121,137) peak is multiplied by the fraction (0.02) of the X-rays that escape. The resulting product is then subtracted from the measured area of the 97 kev. peak. This area is then corrected for the fraction (0.06) of the X rays that escape from the 97 kev. peak. The result is then taken as the actual

area of the 97 kev. photo electric peak, and from which the relative intensity is obtained. Using the corrected photo peak area for the 97 kev. gamma ray the intensity of the 66 kev. gamma ray is obtained in a similar fashion.

BIBLIOGRAPHY

1. Fermi Z.Phys.k. 88, 161, 1934
2. National Bureau of Standards; Tables for the Analysis of Beta Spectra.
3. Moszkowski Phys.Rev. 82, 35 (1951).
4. Rose and Goertzel Appendix IV K.Seighahn and ray Spectroscopy.
5. Frauenfelder page 549 K. Seighahn and ray Spectroscopy.
6. Biedenharn and Rose. Rev.Mod.Phys. 25, 746 (1953).
7. Mayer Phys.Rev. 78, 16, 1950
   Haxel, Jensen Suess Phys.Rev. 75, 1766L (1949)
   Z.Physik. 128, 295, (1950)
8. Bohr and Mottelson Dan.Mat.Fys.Medd. 27 (1953)
   K.Seigbahn and ray spectroscopy (Chap.17)
9. Alder, Bohr, Huus, Mottelson, Winther and Zupancic
   Rev.Mod.Phys. 28, 432, (1956)
10. Goldhaber and Sunyar Phys.Rev. 83, 906, 1951.
11. McMahon Master's Thesis U.B.C.
12. RBR.Bell p.154 K.Seigbahn Beta and Gamma Ray Spectroscopy.
13. Milley Master's Thesis U.B.C.
14. Ter-Pogossian, Robinson and Cook. Phys.Rev. 75, 995 (1949).
15. Cork, Rutledge, Branyan, Stoddard and LeBlanc. Phys.Rev. 79, 889 (1950)
16. Jensen Laslett Martin Hughes and Pratt Phys.Rev.90, 557 (1953).
17. Schardt and Welker Phys.Rev. 99, 810 (1955)
18. Temmer and Heydenburg Phys.Rev. 93, 351 (1954).
19. Lu Kelly and Weidenback Phys.Rev. 97, 139 (1955).
20. Davisson and Evans Rev.Mod.Phys. 24, 79, 1952.
21. Moszkowski Seigbahn Beta and Gamma Ray Spectroscopy, page 391
22. A amodt, Fletcher, Silvey and Townes Phys.Rev. 98, 1224 (1955)
23. Trail and Johnson Phys.Rev. 91. 474 (1953).
24. Klinkenberg Rev.Mod.Phys. 24, 63, (1952).
25. DeBenedett: and McGowan Phys.Rev 74, 728, (1948).
26. Feenberg and Hammack Phys.Rev. 75, 1877 (1949).
27. Nordhiem Phys.Rev. 75, 1894 (1949)
28. Bell, P.R. Seigbahn - Beta and Gamma Ray Spectroscopy, page 139
29. Bell, P.R. loc. cit. page 155.